

Journal: Biochemical Pharmacology
Full Length Research Article

Pancreatic Ductal Adenocarcinoma Cell Secreted Extracellular Vesicles Containing Ceramide-1-Phosphate Promote Pancreatic Cancer Stem Cell Motility

Running head (50 characters): PDAC secreted C1P mediates stem cell migration

Norbert Kuc*¹, Allison Doermann*¹, Carolyn Shirey², Daniel D. Lee^{3,4}, Chinn-Woan Lowe³, Niranjan Awasthi⁵, Roderich E. Schwarz^{5,7}, Robert V. Stahelin^{2,6}, and Margaret A. Schwarz^{2,3,4}

*Co-first authors

Institutions: ¹Department of Biological Sciences University of Notre Dame, ²Department of Chemistry and Biochemistry University of Notre Dame, ³Cellular and Integrative Physiology, ⁴Pediatrics, ⁵Surgery, and ⁶Biochemistry and Molecular Biology, Indiana University School of Medicine, ⁷Goshen Center for Cancer Care, Goshen Indiana.

Author contributions: NK and AD contributed to and performed in vitro experiments, in vivo studies, analyzed and interpreted data, CS performed the C1P translocation studies and DLS analysis, DDL designed experiments, interpreted data, revised the manuscript, and participated in Western Blot and microscopy analysis, CWL performed vesicle isolation and studies, NA and RES provided pancreatic cancer cell expertise and critically reviewed the manuscript, RVS provided C1P expertise and critically reviewed the manuscript, MAS conceived the project, designed experiments, analyzed and interpreted data, and wrote the manuscript.

Correspondence:

Margaret A. Schwarz, MD
Indiana University School of Medicine,
1234 Notre Dame Avenue,
South Bend, Indiana, 46617
E-mail: schwarma@iu.edu

Acknowledgements:

NIH: 5R01HL114977 (MAS), Lilly Endowment Physician Scientist Initiative (MAS), Research like a Champion (NK, AD), Walther Foundation (MAS, RVS), NSF Graduate Research Fellowship DGE-1313583 (CMS), Medical University of South Carolina (MUSC) core facility.^a

Key words: sphingolipids, tumor dissemination, ceramides, Ceramide-1-Phosphate

^a *The content is solely the responsibility of the authors and does not necessarily represent the official views of the National Institutes of Health*

ABSTRACT: (200 words)

The high mortality rate associated with pancreatic ductal adenocarcinoma (PDAC) is in part due to lack of effective therapy for this highly chemoresistant tumor. Cancer stem cells, a subset of cancer cells responsible for tumor initiation and metastasis, are not targeted by conventional cytotoxic agents, which renders the identification of factors that facilitate cancer stem cell activation useful in defining targetable mechanisms. We determined that bioactive sphingolipid induced migration of pancreatic cancer stem cells (PCSC) and signaling was specific to ceramide-1-phosphate (C1P). Furthermore, PDAC cells were identified as a rich source of C1P. Importantly, PDAC cells express the C1P converting enzyme ceramide kinase (CerK), secrete C1P-containing extracellular vesicles that mediate PCSC migration, and when co-injected with PCSC reduce animal survival in a PDAC peritoneal dissemination model. Our findings suggest that PDAC secrete C1P-containing extracellular vesicles as a means of recruiting PCSC to sustain tumor growth therefore making C1P release a mechanism that could facilitate tumor progression.

Highlights:

- PDAC are a source of bioactive sphingolipid C1P
- PDAC secrete C1P-containing vesicles recruit PCSC
- Uptake of PDAC secreted C1P-vesicles in a peri-nuclear region of PCSC
- PDAC and PCSC co-injection reduces animal survival.

1. Introduction: (5,000 words)

Pancreatic cancer, the third leading cause of death in the United States when both genders are combined, is expected to become the second-leading cause of death by 2030 (1). Asymptomatic during early stages, detection of pancreatic cancers remains a challenge as the majority of cases are identified following invasion of adjacent lymph nodes or metastasis to distant sites.

Accounting for ~85% of pancreatic cancers, pancreatic ductal adenocarcinoma (PDAC) is an aggressive tumor of multiple cell lineages composed of complex stromal elements, epithelial adenocarcinoma cells, and cancer stem cells (CSC); it is often fatal with a 5-year survival rate of less than 6% (2). Despite more intense drug regimens, there remains a large gap in improving overall survival of patients with pancreatic cancers due to marked resistance to conventional chemotherapy, rapid growth and progression and high probability of recurrence after resection of apparently localized disease. Identification of additional therapeutic targets is essential to further enhance a targeted-cytotoxic combination strategy for advanced PDAC.

Cancer stem cells, a subset of cancer cells responsible for tumor initiation and metastasis, are not the primary target of conventional chemotherapy. Recently, lipid signaling has been shown to be an important element of the stem cell niche (3) and may represent a novel targeting mechanism of inhibiting CSC migration and proliferation. Bioactive lipids, sphingolipids, are structural components of eukaryotic cell membranes that have key roles in cellular signaling and membrane trafficking. In response to inflammation, cells release bioactive lipids that function locally to mediate local apoptosis, cell growth, and differentiation(4). One such lipid is ceramide, which promotes apoptosis and can induce cell cycle arrest. Ceramide-1-phosphate (C1P), its direct metabolite through phosphorylation by the enzyme ceramide kinase (CerK), has opposite

effects as it has been shown to increase cell proliferation, serve as an anti-inflammatory signal and facilitate cell evasion of apoptosis(5). Found in extracellular fluid, C1P plays a critical role as a chemoattractant in trafficking of normal and stem cell populations(5), however its receptor remains unknown. While recent studies have focused on C1P's impact on hematopoietic CSC migration and proliferation, mechanistically C1P's impact in solid tumors such as pancreatic cancer is poorly understood. In this study, we determined that sphingolipid activation of pancreatic CSC (PCSC) migration and adhesion is C1P specific and selective for PCSC as PDAC cells are unaffected. Reduction in animal survival using an established peritoneal dissemination model when PCSC are co-injected with PDAC cells as well as enhanced PCSC migration in response to PDAC-conditioned medium supports PDAC-facilitated PCSC activation. Localization of both C1P-containing extracellular vesicles in PDAC conditioned medium and labeled C1P to the peri-nuclear region suggest that PDAC cells promote PCSC migration and activation through release of C1P-containing extracellular vesicles.

2. Materials and Methods:

Reagents: Lipids and Topfluor-lipids were acquired from Avanti Polar Lipids (Alabaster, AL). C16 Ceramide-1-Phosphate (d18:1/16:0) (Avanti Polar Lipids, Inc. #860533) or C16 Ceramide (d18:1/16:0) (Avanti Polar Lipids, Inc. #860516) initially were dissolved in chloroform before aliquoting and drying under nitrogen stream. Lipids were reconstituted in 98:2 ethanol:dodecane solution at 100 mM solution resulting in the stock solution having a dodecane/C1P ratio ≈ 1 that is well below the noted toxicity range of dodecane (6) and diluted as noted below. Fibronectin human protein, collagen I rat protein, and laminin mouse protein (natural) were obtained from Life Technologies (St. Petersburg, FL).

Lipidomics analysis: Cells were counted, rinsed in PBS, pelleted and frozen at minus 80 degrees Celsius. Equal cell numbers were analyzed at the Medical University of South Carolina (MUSC) core facility using a MRM transition from molecular weight to 264 amu (sphingoid base backbone) along with chromatographic separation. Standards were utilized for each measurement and extraction was performed using an isopropanol/ethyl acetate extraction method followed by lipid extraction and analysis by HPLC (7, 8). C1P was normalized to total cell number and samples obtained at different passages and on different days.

Cell Culture: Human Pancreatic Cancer Stem Cells purchased from Celprogen (Torrance, CA), grown in Celprogen Complete Growth Medium at 37°C in a humidified 5% CO₂ atmosphere and used between passages 3-9 with Trypsin/EDTA (Celprogen) and split at a 1:3 ratio. Cell phenotype was confirmed prior to use. PDAC Human AsPC-1, CFPAC (human pancreatic ductal adenocarcinoma derived from metastatic origin), and Panc-1 (human pancreatic duct epithelioid carcinoma) cells were obtained from ATCC. AsPC-1 cells were grown in RPMI 1640 medium

(Sigma Chemical, St Louis, MO) supplemented with 10% fetal bovine serum (FBS) and 1% penicillin/streptomycin in a humidified 5% CO₂ atmosphere. Panc-1 and CFPAC cells were grown in DMEM (HyClone, Logan, UT) supplemented with 10% FBS and 1% penicillin/streptomycin in a humidified 5% CO₂ atmosphere.

Conditioned Medium: Some studies were performed using CFPAC-conditioned medium obtained by collecting DMEM off of 80% confluent CFPAC cells after a 24-hour incubation period. Conditioned medium was filtered with a 0.22µm filter (Jet Biofil, Elgin, IL) and mixed 1:1 with fresh DMEM medium for replenishment. For control, un-conditioned CFPAC medium (CFPAC Medium) was used (9, 10).

Hanging Drops: A 3D hanging drop model was used to assess migration via compaction using three dimensional cell spheroids (11-16). Cells were suspended in their respective growth media with vehicle or treatment at a concentration of 2.5×10^6 cells/ml for PCSCs and 1.5×10^6 cells/ml for CFPAC cells. Hanging drops of 12.5µl (31,250 PCSC cells/HD and 18,750 CFPAC cells/HD) were suspended over PBS on the lids of 60 mm Petri dishes. Compaction of cells during self-assembly for 48 hours was assessed in phase contrast images by outlining the cellular mass and measurement of the entire outline of the HD in pixel number as previously described (17).

Scratch Assay: Cell migration was assessed using scratch tests on 12 well 'expansion' plates obtained from Celprogen. Cells were plated at a density of 2.2×10^5 cells per well and allowed to seed for 24 hours, after which a confluent monolayer formed. Each well was scratched with a pipette tip and washed twice with PBS. Wells were then treated with 3 or 10 µM ceramide 1-phosphate, ceramide, or vehicle (98:2 ethanol:dodecane) dilutions from an original 100 mM

stock. Cells were imaged using IX81 Olympus Spinning Confocal microscope images captured with a Hamamatsu Orca-ER Digital camera. Scratches were imaged at 0 hours and 24 hours, and the scratch area was measured using (CellSens software) to determine percent closure.

Co-culture Scratch Test: 0.12×10^6 cells of CFPAC and PCSCs were grown in 6.5mm transwells (VWR, Radnor, PA) for 24 hours. Concurrently, 2.2×10^6 PCSCs were plated onto 12-well plates and allowed to seed for 24 hours. 12-well plates were then scratched, washed 2x with PBS, and new medium was added with treatment or vehicle. Scratches were imaged and transwells containing either CFPACs or PCSCs were added to each well. PCSC transwells were added to vehicle and C1P treated wells, whereas CFPAC transwells were added to the CFPAC condition. After 24 hours transwells were removed and scratches were imaged and assessed for percent closure.

Adhesion Assay: Non-tissue culture treated 96-well plates (Sigma-Aldrich) were coated with 1, 3, or 10 μg of laminin (LA), collagen (type I) (CL), or fibronectin (FN). ECM proteins dissolved in CAPS buffer (carbonate-bicarbonate buffer) for plate coating. Some wells were treated with 10 μM ceramide or C1P. Treated plates were then incubated at 4 $^{\circ}\text{C}$ overnight to allow for coating. Coating treatment was removed and wells were washed three times with PBS before adding cells (0.4×10^4 cells per well). Plates were treated with 1% BSA for one hour, then washed three times. The assay was performed with PCSCs and CFPAC cells. CFPAC cells were allowed to adhere at 37 $^{\circ}\text{C}$ in a humidified 5% CO_2 atmosphere for 2.5-4 hours, whereas PCSCs were allowed to adhere for 1-2 hours, depending on ECM type. After cell adherence, wells were washed twice and then treated with crystal violet with standard protocol. Crystal violet was solubilized using 10% (v/v) acetic acid. Plate was read at 570 nm.

Vesicle isolation: Cells grown to 70% confluence were rinsed with PBS and incubated with serum-free (SF) complete medium for 24 hours. Supernatant was collected and added drop wise into an ultracentrifuge tube containing STE with 20% sucrose. Cellular debris was removed by spinning the cells down for 30 min at 10,000 g. The supernatant was transferred to a new tube and spun for 90 min at 100,000g. Vesicles were resuspended in PBS. Some were surface labeled with PKH26 red fluorescent dye (Sigma) for visualization while others were sent for lipidomic analysis (MUSC). All samples were normalized to total phosphate (Pi) (nmole/sample) and all samples obtained at different passages and on different days.

Western Blot: 1×10^6 PCSCs were plated on 12 well plates and allowed to grow for 24 hours. Medium was then replaced with serum-free medium and allowed to incubate for a further 24 hours for serum-starving. Following serum starvation, PCSCs were exposed to $3\mu\text{M}$ C1P, $3\mu\text{M}$ ceramide, or 1:1 CFPAC conditioned:fresh DMEM. All treatments were delivered via serum-free DMEM. Treatments were allowed to incubate for 5, 10, or 30 minutes before the treatment was removed. Plates were placed on ice and washed 2x with ice-cold PBS. Ice-cold lysis buffer was added and allowed to incubate for 15 minutes under constant agitation. Each well was subsequently scraped before the lysates were harvested. Lysates were centrifuged at max speed (14,000 rpm) for 10 minutes. The supernatant was transferred to fresh 1.5ml tubes, LDS was added, and lysates were incubated at 70°C for 10 minutes before loading onto 12% Bis-Tris gels. Western blots were probed for CerK, p42/44 MAPK, and total MAPK. Alpha-tubulin was used as a loading control.

Dynamic Light Scattering (DLS): CFPAC conditioned medium was collected, vesicles isolated, as described above and analyzed by DLS. Vesicles preparations were characterized on a Nano Series Zetasizer (zetasizer, Malvern Instruments, Southborough, MA) (DLS; He-Ne laser, 633

nm; 173°backscattered light detection). Performed at 25 °C, each measurement represents 4 unique preparations, 3 runs per preparation and a minimum of 12 measurements per run for a total of 144 measurements.

Animal Studies: In accordance with the Institutional Animal Care and Use Committee (IACUC) at the Indiana University School of Medicine (South Bend, IN) animals were housed in a pathogen-free facility with access to food and water *ad libitum*. Survival studies were performed using female nonobese diabetic/severe combined immunodeficient (NOD/SCID) mice as previously described (18, 19). Mice were intraperitoneally injected with AsPC-1 cells (0.75×10^6), ASPC-1 (0.75×10^6), + PCSC cells (0.75×10^6): 1:1 ratio, ASPC-1 (0.75×10^6), + PCSC cells (1.5×10^6): 1:2 ratio, or PCSC cells alone (0.75×10^6). Animals were euthanized when moribund according to predefined criteria (19). Animal survival was evaluated from the first day of injection until death.

Confocal Microscopy: For imaging experiments, cells were seeded in Nunc Lab-Tek™ II 8-well imaging plates (Fisher Scientific) in growth medium, grown to ~70% confluency and treated with either TopFluor-C1P (C11 TopFluor®Ceramide-1-phosphate: Avanti Polar Lipids, Inc. #810270) or TopFluor-Ceramide (C11 TopFluor® Ceramide: Avanti Polar Lipids, Inc., #810262). Lipid was prepared by adding the required amount of stock lipid into a glass vial and dried under a stream of N₂. Lipid was re-suspended in ethanol:dodecane (98:2) (Wijesinghe et al., 2009) to a concentration of 100 μM, followed by sonication for ten cycles of 10 s on, 10 s off, followed by incubation in 37°C for 20 minutes. Lipids were added to cells in 8-well imaging plates to a final concentration of 1 μM. Cells were image using confocal microscopy (Zeiss LSM 710) using an oil 630x 1.4 numerical aperture objective. TopFluor excitation was at 488 nm with emission measured using green fluorescent protein (GFP) settings from 510 to 600 nm.

3. Results:

Sphingolipid mediated PCSC migration is Ceramide-1-phosphate specific. Bioactive sphingolipids regulate hematopoietic stem cell proliferation and migration, however little is known regarding the impact of sphingolipids on pancreatic cancer stem cells. PDAC cell migration *in vitro* is modulated by CerK expression, a key mediator of ceramide phosphorylation to C1P (20), however C1P levels in PDAC cells have not been explored. Lipidomic analysis identified a marked increase in C1P species in pancreatic adenocarcinoma cells, CFPAC, as compared to PCSC cells. Specifically, statistically significant increases were detected d18:1/18:0-C1P, d18:1/18:1-C1P, and d18:1/20:0-C1P in CFPAC versus PCSC (Figure 1). Although d18:1/16:0-C1P species was more highly expressed in CFPAC cells versus PCSC, it did not reach statistical significance. To determine PCSC cell responsiveness, C1P dosing known to mediate hematopoietic progenitor cell recruitment were explored (3, 21). The impact of sphingolipids lipid-mediated cell migration was screened using a 3-dimensional (3D) compaction assay that measures cell-cell interactions and cellular rearrangement. A decreased diameter reflecting a more compact spheroid and enhanced migration. C1P enhanced PCSCs migration while other sphingolipid metabolites such as ceramide, sphingosine or sphingosine-1-phosphate had no impact (Figure 2A,B). Increased compaction in response to C1P was specific to PCSC cells, as no other tested sphingolipids impacted sphere formation of the PDAC cell lines CFPAC, and Panc-1 cells (Figure 2C,D). Conventional two-dimensional migration study in form of a scratch assay confirmed C1P-specific mediation of PCSC migration (Figure 2E). Absence of Ki67 staining at the leading edge of the wound (Fig. 2F, white line denotes leading wound edge, white arrows define Ki67 positive cells) verified that cell migration, not proliferation, was responsible for wound closure. Consistent with these findings, C1P had no impact on PCSC or

CFPAC cell proliferation (Figure 3A) while C1P induced MAPK phosphorylation with dominance of the p42MAPK isoform at 5 and 10 minutes in a time-dependent manner (Figure 3B).

C1P-enhanced PCSC adhesion is fibronectin specific. As cell migration is modulated in part by cell-cell mutual bonding and adhesive free energy, the impact of C1P on adhesion was explored. Although PCSC demonstrated a dose-dependent binding to FN, CL, and LA (Figure 4A,B, and C respectively), addition of C1P enhanced only PCSC FN-dependent adhesion (Figure 4A). Interestingly, C1P had no impact on PDAC adhesion to CL or LA (Figure 4D, E). PDAC cells did not adhere to FN.

PCSC cells interact with PDAC in an in vivo peritoneal dissemination model and in an in vitro migration and activation. Although human PDAC tumor growth in an animal survival peritoneal dissemination model replicates the clinical progression of pancreatic cancer (18), little is known regarding the role of PCSC in disease progression. Using PDAC AsPC-1 cells alone or in combination with PCSC cells, tumor cells were injected intraperitoneally and animal survival was monitored within the groups from time of tumor cell injection. Median survival in AsPC-1 cells alone was 40 days, consistent with previous studies (18, 22-24) (Figure 5A).

Intraperitoneal PCSC cells resulted in no tumor growth and had no impact on survival at 80 days post-injection (Figure 5A, $p \leq 0.0001$ as compared to AsPC-1). However, mixed injection of PCSC and PDAC AsPC-1 cells at ratios of 1:1 or 1:2 markedly shortened survival [median survival at 29 and 33 days, respectively, a 33% ($p=0.0006$) or 28% ($p=0.0023$) decrease in survival] as compared to ASPC cells alone (40-day survival median time from tumor cell injection) suggesting a dynamic interaction between the two cell populations. In vitro analysis determined that CFPAC-conditioned medium as well as transwell co-culture of CFPAC cells

with PCSC cells enhanced PCSC cell migration consistent with C1P (Figure 5B,C) as compared to vehicle or un-conditioned CFPAC medium (CFPAC Medium, Figure 5B). Similar to C1P, CFPAC-conditioned medium induced a rapid, robust MAPK phosphorylation, with dominance of the p42 MAPK isoform between 5 and 10 minutes of exposure (Figure 5D). Of note, CFPAC-conditioned medium induced a greater effect on pMAPK and migration than C1P alone suggesting that other components are present in the conditioned medium that influence these parameters.

C1P-rich PDAC secrete extracellular vesicles containing C1P whose peri-nuclear uptake by PCSC is consistent with that seen in TopFluor labeled C1P. Decreased survival by co-injection with PDAC/PCSC cells, increased MAPK phosphorylation in PCSC by conditioned PDAC medium, and enhanced migration of PCSC in PDAC transwell studies suggest that CFPAC cell secretion of a mediating factor promotes PCSC activation. Dynamic Light Scattering (DLS) analysis of extracellular vesicles isolated from serum-free CFPAC condition medium subjected to a sucrose gradient determined that 95.88% of the vesicles were $116\text{nm} \pm 3.5\text{ SEM}$ in size (Figure 6B). Lipidomic analysis determined that extracellular vesicles are C1P-containing with d18:1/18:0 as the predominant C1P species (Figure 6C). Consistent with secreted C1P-containing vesicles, CFPAC cells in serum-free medium demonstrated an increase in the ceramide to ceramide-1-phosphate converting enzyme CERK as compared to normal medium (Figure 6D). CFPAC cells demonstrate minimal uptake of either fluorescent conjugated TopFluor-C1P or TopFluor-ceramide (Figure 6E,F). In contrast, PCSC cells have a marked peri-nuclear focal uptake of TopFluor-C1P while minimal TopFluor-ceramide was transported intracellularly (Figure 6H,I respectively). Consistent with PCSC peri-nuclear uptake of

TopFluor-C1P, CFPAC secreted extracellular vesicles surface-labeled with a fluorescent dye were taken up in a focal peri-nuclear pattern in PCSC cells (Figure 6J).

ACCEPTED MANUSCRIPT

4. Discussion:

Cancer stem cells have a vital role in tumor initiation, growth, and metastasis. Identification of factors that modulate cancer stem cell recruitment is highly relevant to effectively treat aggressive and chemo-resistant pancreatic ductal adenocarcinomas. Bioactive sphingolipids, sphingosine-1-phosphate (S1P) and ceramide-1-phosphate (C1P) have recently been identified as key mediators of stem cell mobilization, homing, metastasis, and activation (25). In this report, we demonstrate for the first time that C1P is a modulator of PCSC migration, and fibronectin specific based adhesion. Furthermore, we show that co-injection of PCSCs with PDAC cells reduce survival in a peritoneal dissemination animal model. Importantly, PDAC cells were identified as a source of C1P, conditioned medium from PDAC cells can simulate C1P-induced PCSC migration and signaling, and they secrete extracellular vesicles containing C1P. Taken together these studies support a role for PDAC modulation of PCSC through a C1P-mediated mechanism.

Ceramide, long identified as a signaling molecule adept at regulating key cellular functions, effectively inhibits cell survival (26). In contrast, conversion of ceramide to ceramide-1-phosphate through ceramide kinase (CerK) supports tissue regeneration, in part through endothelial progenitor cell chemoattraction. Elevated in damaged tissues following injury, a role for C1P in supporting tissue regeneration has been identified in the wound healing process. For example, elevation of C1P is associated with improved mobilization of circulating progenitor cells in cardiovascular disease (27), enhanced fibroblast migration in wound healing (28), and in spinal cord injury, C1P contributes to repair following injury (29, 30). In these studies, improvement in wound healing was in part attributed to C1P's potential to recruit endothelial and neural stem cells. Other studies noted that progenitor cell responsiveness was sphingolipid

specific as endothelial cell migration and regeneration are C1P specific (21) whereas both S1P and C1P impact multipotent stromal cell differentiation and proliferation (25). Similar processes could be employed by the tumor microenvironment to enhance growth and meet its metabolic demands. The role of C1P in tumor formation has not been extensively explored. However, a link between elevated S1P and C1P plasma levels in response to radio/chemotherapy in patients with rhabdomyosarcoma and the association of increased metastatic lesions suggests that sphingolipids facilitate a ‘prometastatic microenvironment’ (31).

Interestingly, our observation that PDAC cells secrete C1P-containing vesicles supports the notion that C1P secretion could be an important mechanism of cell specific recruitment and activation of progenitor cells. In line with the concept that C1P promotes a ‘prometastatic microenvironment’, recent *in vitro* tumor cell invasion studies using PDAC cells determined that C1P impacts tumor cell mobility (20).

In our studies, although other sphingolipids had minimal impact on the number of migrating PDAC cells, the magnitude of PCSC responsiveness specifically to C1P suggests it has the ability to recruit pancreatic cancer stem cells. Furthermore, our studies determined that PDAC cells are a rich source of C1P. In conjunction with elevated C1P levels in PDAC cells, CerK expression, a known enhancer in the conversion of ceramide to C1P is elevated in PDAC cells consistent with our findings has been previously reported (20). This is particularly important as CerK expression impacts recruitment of progenitor cell populations and tumor growth and when elevated in breast cancer was found to be associated with recurrence and tumor cell survival (32). Interestingly, our studies observed that during the stress of serum-free conditions, PDAC cells demonstrate an increase in CerK. Although this remains to be tested, this suggests that in PDAC cells, elevated CerK levels could contribute to the enzymatic conversion of ceramide to C1P and

is a focus of our future studies. Previous studies have explored C1P levels in healthy and pathologic states to determine if there is an association between elevated C1P and disease progression. Although the levels of C1P found in serum and plasma of healthy individuals were (0.5 μ M) (33) and isolates from irradiated mice demonstrate variable organ levels of C1P (2.12 μ M/nM total phosphate in liver and 0.058 μ M/nM total phosphate in lung) (31), less is known regarding average C1P levels found in tumor cells. In this study, we determined that CFPAC cell C1P levels were species dependent. With the d18:1/16:0 C1P being the most prevalent species (Figure 1). These finding suggests that C1P and its biological influences are more complex than previously known. With C1P being released into the tumor microenvironment through secretion in extracellular vesicles, this C1P-rich tumor microenvironment could represent one method of PDAC cell mediated recruitment of the stem cells necessary to support the evolving tumor progression needs. Therefore, it is plausible that as the tumor needs escalate, one way to influence stem cell recruitment could be in part through CerK-mediated conversion of ceramide to C1P and subsequent release of C1P in extracellular vesicles into the tumor microenvironment. One such cell population is endothelial progenitor cells. Recent studies support a role for C1P-mediated recruitment of progenitor endothelial cells as a mechanism of promoting vascularization (21). In the context of ever-expanding tumor nutritional and metabolic requirements, release of C1P by tumor cells could represent one mechanism of tumor tissue recruitment of progenitor endothelial cell populations that can contribute to tumor vessel formation. Importantly, vessel growth is in part facilitated by adhesion of endothelial cells to fibronectin. Our studies determined that C1P-enhanced PCSC adhesion only to fibronectin while other extracellular matrix such as collagen and laminin were not impacted by C1P. These findings suggest that in the tumor microenvironment, C1P not only

recruits progenitor CSC but also facilitates their adhesion. Previous studies explore the role of non-vesicular C1P following tissue damage that establishes a gradient responsible for stem cell recruitment (21). Our findings suggest that tumor cells secrete C1P-containing vesicles that facilitate stem cell migration in part through ERK activation. Importantly, as vesicles have been associated with additional intraluminal cargo that can impact cellular function including microRNA, proteins, peptides, and nucleic acids, future studies are necessary to explore the role of C1P in the fate of extracellular vesicles and their cargo (34). Taken together, our findings suggest a mechanism that should be explored as a potential therapeutic target to reduce tumor progression.

Our findings support a role for sphingolipid C1P-mediated PCSC migration, adhesion, and MAPK phosphorylation. Furthermore, we identified a potential C1P source as C1P rich PDAC cells release C1P-containing vesicles. Regulation of the enzymatic conversion in PDAC cells of ceramide to ceramide-1-phosphate could minimize stem cell recruitment and may represent a mechanism that could reduce pancreatic tumor progression.

Acknowledgments: This publication was made possible in part by 5R01HL114977 (MAS) from NIH, the Lilly Endowment, Inc. Physician Scientist Initiative (MAS), Walther Foundation Grant (MAS and RVS), NSF Graduate Research Fellowship DGE-1313583 (CMS), MUSC core facility and Research Like a Champion (AD and NK).

Conflict of interest statement: The authors have declared that no conflict of interest exists.

Figure Legends:

Figure 1: CFPAC cells are C1P rich. Subconfluent CFPAC and PCSC cells were sent for analysis of C1P. Lipidomic analysis of C1P normalized to the specific species standard curve, determined that C1P species d18:1/18:0-C1P (CFPAC: $41\mu\text{m} \pm 10\text{SEM}$; PCSC: $4.3\mu\text{m} \pm 0.2\text{SEM}$, * $p < 0.007$), d18:1/18:1-C1P (CFPAC: $48.3\mu\text{m} \pm 9\text{SEM}$; PCSC: $5.8\mu\text{m} \pm 0.7\text{SEM}$, ** $p = 0.002$), and d18:1/20:0-C1P (CFPAC: $18.8\mu\text{m} \pm 3.6\text{SEM}$; PCSC: $0.5\mu\text{m} \pm 0.1\text{SEM}$, * $p < 0.007$) were significantly increased in CFPAC versus PCSC (unpaired Student's *t*-test, $n = 3$ /experiments performed on different cell passages harvested at different times and normalized to total cell number) (nomenclature: Sphingosine backbone of C1P is - 18:1).

Figure 2: C1P mediated migration is selective to pancreatic cancer stem cells. Single cell suspensions of PCSC, CFPAC, and PANC1 in three-dimensional screening migration assay were assessed for aggregation at 48 hours with a decreased diameter reflecting a more compact spheroid and enhanced migration (measured as pixels). PCSC treated with C1P exhibited significant compaction (B, $3\mu\text{M}$: $1.09 \times 10^6 \pm 5.66 \times 10^4$ SEM pixels and $10\mu\text{M}$: $9.01 \times 10^5 \pm 2.1 \times 10^4$ SEM pixels) ($p \leq 0.0001$) (unpaired Student's *t*-test, $n = 10$ /condition/experiment performed a minimum of 5 times) as compared to vehicle ($1.97 \times 10^6 \pm 3.17 \times 10^4$ SEM pixels).

Compaction was specific to C1P as ceramide (cer) (A, $10\mu\text{M}$: $2.14 \times 10^6 \pm 5.79 \times 10^4$ SEM pixel, B, $3\mu\text{M}$: $1.88 \times 10^6 \pm 10.8 \times 10^4$ SEM pixels and $10\mu\text{M}$: $1.73 \times 10^6 \pm 10.6 \times 10^4$ SEM pixels), S1P (A, $10\mu\text{M}$: $2.25 \times 10^6 \pm 4.8 \times 10^4$ SEM pixels) or sphingosine (Sph) (A, $10\mu\text{M}$: $2.38 \times 10^6 \pm 2.5 \times 10^4$ SEM pixels) had no impact on PCSC aggregation. C1P had no impact on Panc1 or CFPAC cell aggregation (C, D respectively). Confluent monolayers subjected to *in vitro* scratch

assay were assessed for wound closure at 24 hours. PCSC treated with C1P had a 41% (E, 10 μ M: 41% \pm 2.7 SEM closure)(p=0.005)(ANOVA with post-hoc comparison, n=3/condition/experiment performed a minimum of 5 occasions) as compared to vehicle (E, 26% \pm 1.7 SEM closure) and ceramide (10 μ M: 25% \pm 0.4 SEM closure). Ki67 immunofluorescence staining (Cy3) at wound leading edge (white dotted line) supports wound closure in C1P treated cells is predominately due to migration (F). C1P and ceramide had no impact on CFPAC wound closure (G).

Figure 3: C1P had no impact on CSC or CFPAC proliferation, but does induce MAPK phosphorylation in CSC cells. Proliferation using WST in subconfluent CSC or CFPAC cells was not influenced by C1P (1-10 μ M) or ceramide (1-10 μ M) (A). Subconfluent PCSC cells were assessed for phosphorylation of MAPK overtime determined that C1P selectively induced significant phosphorylation as compared to ceramide (B, n=3, three different occasions, p=0.0003, Two-way ANOVA).

Figure 4: C1P increases FN-mediated PCSC adhesion. Wells coated with fibronectin (FN, 1-10 μ M), collagen (CL, 1-10 μ M), laminin (LA, 1-10 μ M), or vehicle (CAPS) as indicated while some wells were dual-coated with C1P (10 μ M) or ceramide (10 μ M). PCSC or CFPAC cells were seeded on pre-coated plates and adherent cells identified by crystal violet staining. PCSC cells demonstrated dose-dependent adhesion to FN (A), CL (B) and LA (C). CFPAC cells were non-adherent to FN (data not shown) but demonstrated a dose-dependent adhesion to CL (D). C1P significantly enhanced PCSC adhesion to 10 μ M FN (A, 0.6145 \pm 0.0272 SEM) (p=0.04,

n=4/condition/experiment performed a minimum of 4 occasions) as compared to 10 μ M FN alone (0.4563 ± 0.0570 SEM) or ceramide + 10 μ M FN (0.3440 ± 0.0032 SEM).

Figure 5: CSCs co-injected with AsPC-1 cells reduces animal survival while CFPAC conditioned medium and CFPAC in transwells increased CSC migration. Studies using AsPC-1 cells (0.75×10^6), AsPC-1 (0.75×10^6), + CSC cells (0.75×10^6), AsPC-1 (0.75×10^6), + CSCs (1.5×10^6), or CSCs alone (0.75×10^6) were injected intraperitoneally into NOD/SCID mice. Survival from was noted from time of tumor cell injection. Statistical group differences in survival time were calculated using log rank testing (Mantel-Cox) with reduction in survival noted in combined injected cell populations PCSC / AsPC-1 (1:1- $p=0.0006$ and 1:2- $p=0.0023$) as compared to AsPC-1 cells alone (A). Study was concluded on day 80 with no loss of CSC injected animals ($p=0.0001$, A) ($n=6$ /group). Consistent with C1P enhanced migration (A, $*p=0.0184$, $45\% \pm 0.43$ SEM), CSCs treated with CFPAC-conditioned medium (B, $**p=0.0025$, $59\% \pm 2.5$ SEM) significantly increased wound closure in CSC scratch assays as compared to unconditioned CFPAC medium ($23\% \pm 1.1$ SEM) or control medium ($36\% \pm 2.2$ SEM) (B, $n=3$ /condition/experiment performed a minimum of 4 occasions). Transwell co-culture of CFPAC cells with wounded CSCs significantly enhanced wound closure (B, $**p=0.00471$, $43\% \pm 2.6$ SEM) consistent with that seen with C1P (B, $*p=0.0035$, $46\% \pm 6.2$ SEM) as compared to control (C, $19\% \pm 3.3$ SEM) ($n=4$ /condition/experiment performed a minimum of 3 occasions). CFPAC-conditioned medium induced a similar pattern of MAPK phosphorylation with densitometry analysis indicating a 5-fold increase in pMAPK (D, $n=2$, two different occasions, representative blot).

Figure 6: Extracellular vesicles secreted in CFPAC-conditioned medium are rich in C1P and C1P uptake is peri-nuclear in progenitor cells and is similar to uptake of CFPAC secreted C1P-containing extracellular vesicles. The size of vesicles isolated using a sucrose gradient from CFPAC conditioned medium were assessed using Dynamic Light Scattering (DLS) where 95.88% were found to be $116\text{nm} \pm 3.5$ SEM in size while the remaining 4.125% were $4219\text{nm} \pm 11.7$ SEM (B) (n=4 unique preparations, 3 runs per preparation and a minimum of 12 measurements per run for a total of 144 measurements). Secreted vesicle isolates from serum-free (SF) CFPAC cells were noted to contain C1P species consistent with that seen in whole cell lysate (normalized to total phosphate: Pi, nmole/sample) (C). CFPAC cells in serum-free (SF) medium by densitometry analysis have a 1.48 increase in CERK compared to cells in normal medium (N) (D, n=2, representative blot). TopFluor labeled ceramide and C1P lipid uptake in sub-confluent PCSC and CFPAC cells. PCSCs exhibit a marked increase in C1P uptake in the perinuclear region (I) as compared to CFPAC (F) or TopFluor-ceramide (H,E). Conditioned medium from CFPAC cells was collected; extracellular vesicles isolated and surfaced labeled (A, PKH26 red fluorescent dye) and added to subconfluent cells (n=3 on different occasions). Perinuclear uptake of extracellular vesicles was significantly greater in PCSCs (J) as compared to CFPAC cells (G) (G,J: DAPI staining denotes nucleus) (n=3 on different occasions). Scale bar: $10\mu\text{m}$ (E,F,H,I), $20\mu\text{m}$ (G,J).

References:

1. Siegel R, Ma J, Zou Z, Jemal A. Cancer statistics, 2014. *CA Cancer J Clin.* 2014;64(1):9-29.
2. Burris HA, 3rd, Moore MJ, Andersen J, Green MR, Rothenberg ML, Modiano MR, et al. Improvements in survival and clinical benefit with gemcitabine as first-line therapy for patients with advanced pancreas cancer: a randomized trial. *J Clin Oncol.* 1997;15(6):2403-13.
3. Hankins JL, Ward KE, Linton SS, Barth BM, Stahelin RV, Fox TE, et al. Ceramide 1-phosphate mediates endothelial cell invasion via the annexin a2-p11 heterotetrameric protein complex. *J Biol Chem.* 2013;288(27):19726-38.
4. Maceyka M, Spiegel S. Sphingolipid metabolites in inflammatory disease. *Nature.* 2014;510(7503):58-67.
5. Presa N, Gomez-Larrauri A, Rivera IG, Ordonez M, Trueba M, Gomez-Munoz A. Regulation of cell migration and inflammation by ceramide 1-phosphate. *Biochim Biophys Acta.* 2016;1861(5):402-9.
6. Tauzin L, Graf C, Sun M, Rovina P, Bouveyron N, Jaritz M, et al. Effects of ceramide-1-phosphate on cultured cells: dependence on dodecane in the vehicle. *J Lipid Res.* 2007;48(1):66-76.
7. Bielawski J, Pierce JS, Snider J, Rembiesa B, Szulc ZM, Bielawska A. Comprehensive quantitative analysis of bioactive sphingolipids by high-performance liquid chromatography-tandem mass spectrometry. *Methods Mol Biol.* 2009;579:443-67.
8. Bielawski J, Pierce JS, Snider J, Rembiesa B, Szulc ZM, Bielawska A. Sphingolipid analysis by high performance liquid chromatography-tandem mass spectrometry (HPLC-MS/MS). *Adv Exp Med Biol.* 2010;688:46-59.
9. Lo Furno D, Mannino G, Giuffrida R, Gili E, Vancheri C, Tarico MS, et al. Neural differentiation of human adipose-derived mesenchymal stem cells induced by glial cell conditioned media. *J Cell Physiol.* 2018;233(10):7091-100.
10. Urata S, Izumi K, Hiratsuka K, Maolake A, Natsagdorj A, Shigehara K, et al. C-C motif ligand 5 promotes migration of prostate cancer cells in the prostate cancer bone metastasis microenvironment. *Cancer Sci.* 2018;109(3):724-31.
11. Foty RA, Forgacs G, Pflieger CM, Steinberg MS. Liquid properties of embryonic tissues: Measurement of interfacial tensions. *Phys Rev Lett.* 1994;72(14):2298-301.
12. Foty RA, Pflieger CM, Forgacs G, Steinberg MS. Surface tensions of embryonic tissues predict their mutual envelopment behavior. *Development.* 1996;122(5):1611-20.
13. Foty RA, Steinberg MS. The differential adhesion hypothesis: a direct evaluation. *Dev Biol.* 2005;278(1):255-63.
14. Robinson EE, Zazzali KM, Corbett SA, Foty RA. Alpha5beta1 integrin mediates strong tissue cohesion. *J Cell Sci.* 2003;116(Pt 2):377-86.
15. Steinberg MS. On the Mechanism of Tissue Reconstruction by Dissociated Cells, Iii. Free Energy Relations and the Reorganization of Fused, Heteronomic Tissue Fragments. *Proc Natl Acad Sci U S A.* 1962;48(10):1769-76.
16. Schwarz MA, Zheng H, Legan S, Foty RA. Lung self-assembly is modulated by tissue surface tensions. *Am J Respir Cell Mol Biol.* 2011;44(5):682-91.
17. Legan SK, Lee DD, Schwarz MA. alpha5beta1 integrin mediates pulmonary epithelial cyst formation. *Dev Dyn.* 2017;246(6):475-84.

18. Schwarz RE, McCarty TM, Peralta EA, Diamond DJ, Ellenhorn JD. An orthotopic in vivo model of human pancreatic cancer. *Surgery*. 1999;126(3):562-7.
19. Awasthi N, Hinz S, Brekken RA, Schwarz MA, Schwarz RE. Nintedanib, a triple angiokinase inhibitor, enhances cytotoxic therapy response in pancreatic cancer. *Cancer Lett*. 2015;358(1):59-66.
20. Rivera IG, Ordonez M, Presa N, Gangoiti P, Gomez-Larrauri A, Trueba M, et al. Ceramide 1-phosphate regulates cell migration and invasion of human pancreatic cancer cells. *Biochem Pharmacol*. 2016;102:107-19.
21. Kim C, Schneider G, Abdel-Latif A, Mierzejewska K, Sunkara M, Borkowska S, et al. Ceramide-1-phosphate regulates migration of multipotent stromal cells and endothelial progenitor cells--implications for tissue regeneration. *Stem Cells*. 2013;31(3):500-10.
22. Awasthi N, Schwarz MA, Schwarz RE. Combination effects of bortezomib with gemcitabine and EMAP II in experimental pancreatic cancer. *Cancer Biol Ther*. 10(1).
23. Awasthi N, Yen PL, Schwarz MA, Schwarz RE. The efficacy of a novel, dual PI3K/mTOR inhibitor NVP-BE235 to enhance chemotherapy and antiangiogenic response in pancreatic cancer. *J Cell Biochem*. 113(3):784-91.
24. Awasthi N, Zhang C, Schwarz AM, Hinz S, Schwarz MA, Schwarz RE. Enhancement of nab-paclitaxel antitumor activity through addition of multitargeting antiangiogenic agents in experimental pancreatic cancer. *Mol Cancer Ther*. 2014;13(5):1032-43.
25. Marycz K, Smieszek A, Jelen M, Chrzastek K, Grzesiak J, Meissner J. The effect of the bioactive sphingolipids S1P and C1P on multipotent stromal cells--new opportunities in regenerative medicine. *Cell Mol Biol Lett*. 2015;20(3):510-33.
26. Gomez-Munoz A. Ceramide 1-phosphate/ceramide, a switch between life and death. *Biochim Biophys Acta*. 2006;1758(12):2049-56.
27. Hayek SS, Klyachkin Y, Asfour A, Ghasemzadeh N, Awad M, Hesaroiieh I, et al. Bioactive Lipids and Circulating Progenitor Cells in Patients with Cardiovascular Disease. *Stem Cells Transl Med*. 2017;6(3):731-5.
28. Wijesinghe DS, Brentnall M, Mietla JA, Hoeflerlin LA, Diegelmann RF, Boise LH, et al. Ceramide kinase is required for a normal eicosanoid response and the subsequent orderly migration of fibroblasts. *J Lipid Res*. 2014;55(7):1298-309.
29. Jones ZB, Ren Y. Sphingolipids in spinal cord injury. *Int J Physiol Pathophysiol Pharmacol*. 2016;8(2):52-69.
30. Qi ZP, Wang GX, Xia P, Hou TT, Zhou HL, Wang TJ, et al. Effects of microtubule-associated protein tau expression on neural stem cell migration after spinal cord injury. *Neural Regen Res*. 2016;11(2):332-7.
31. Schneider G, Bryndza E, Abdel-Latif A, Ratajczak J, Maj M, Tarnowski M, et al. Bioactive lipids S1P and C1P are prometastatic factors in human rhabdomyosarcoma, and their tissue levels increase in response to radio/chemotherapy. *Mol Cancer Res*. 2013;11(7):793-807.
32. Payne AW, Pant DK, Pan TC, Chodosh LA. Ceramide kinase promotes tumor cell survival and mammary tumor recurrence. *Cancer Res*. 2014;74(21):6352-63.
33. Hammad SM, Pierce JS, Soodavar F, Smith KJ, Al Gadban MM, Rembiesa B, et al. Blood sphingolipidomics in healthy humans: impact of sample collection methodology. *J Lipid Res*. 2010;51(10):3074-87.
34. van Niel G, D'Angelo G, Raposo G. Shedding light on the cell biology of extracellular vesicles. *Nat Rev Mol Cell Biol*. 2018;19(4):213-28.

Figure 1

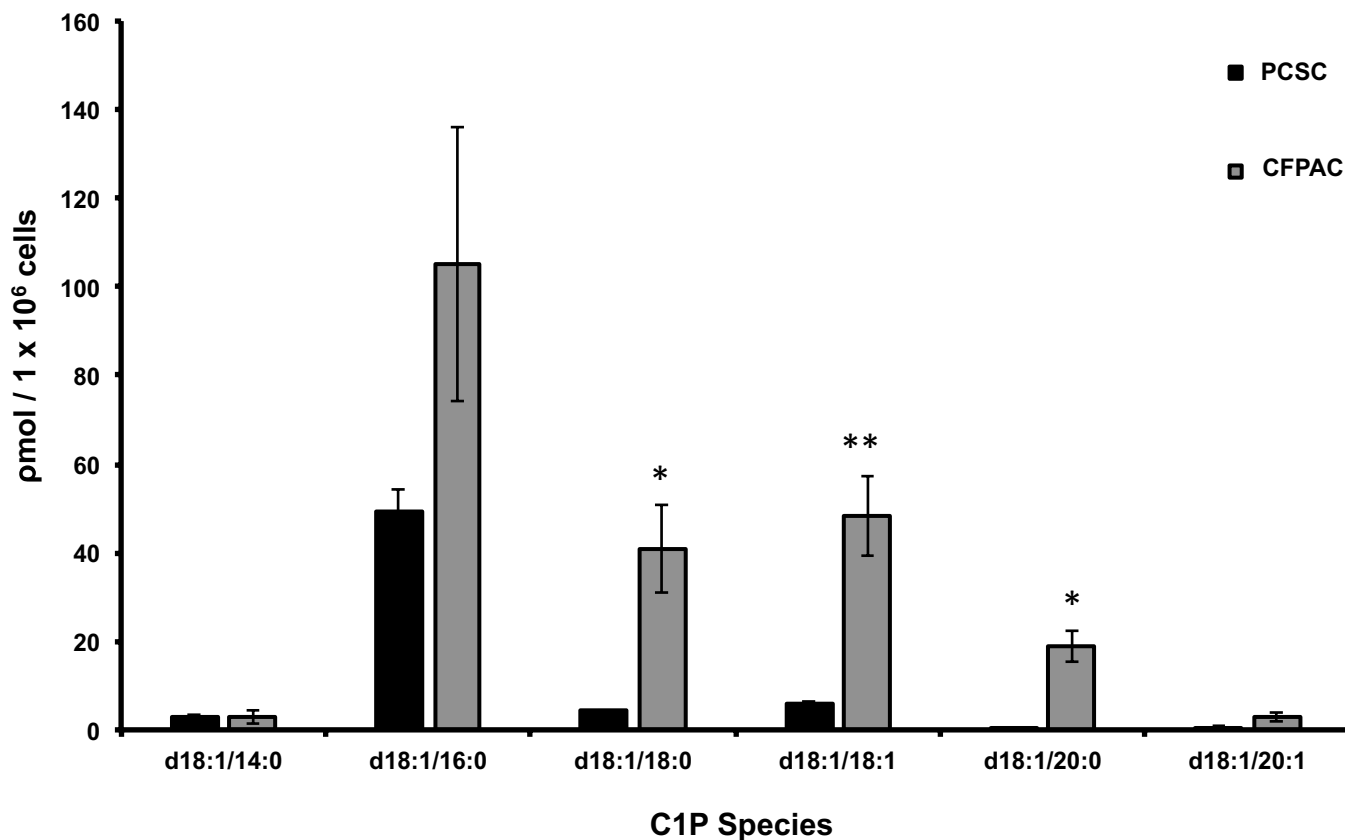


Figure 1: CFPAC cells are C1P rich. Subconfluent CFPAC and PCSC cells were sent for analysis of C1P. Lipidomic analysis of C1P normalized to the specific isoforms standard curve, determined that C1P species d18:1/18:0-C1P (CFPAC: 41pm ± 10SEM; PCSC:4.3pm ± 0.2SEM, * p<0.007) , d18:1/18:1-C1P (CFPAC: 48.3pm ± 9SEM; PCSC:5.8pm ± 0.7SEM, ** p=0.002), and d18:1/20:0-C1P (CFPAC: 18.8pm ± 3.6SEM; PCSC:0.5pm ± 0.1SEM, * p<0.007) were significantly increased in CFPAC versus PCSC (unpaired Student's t-test, n= 3/experiments performed on different cell passages harvested at different times and normalized to total cell number) (nomenclature: Sphingosine backbone of C1P is - 18:1).

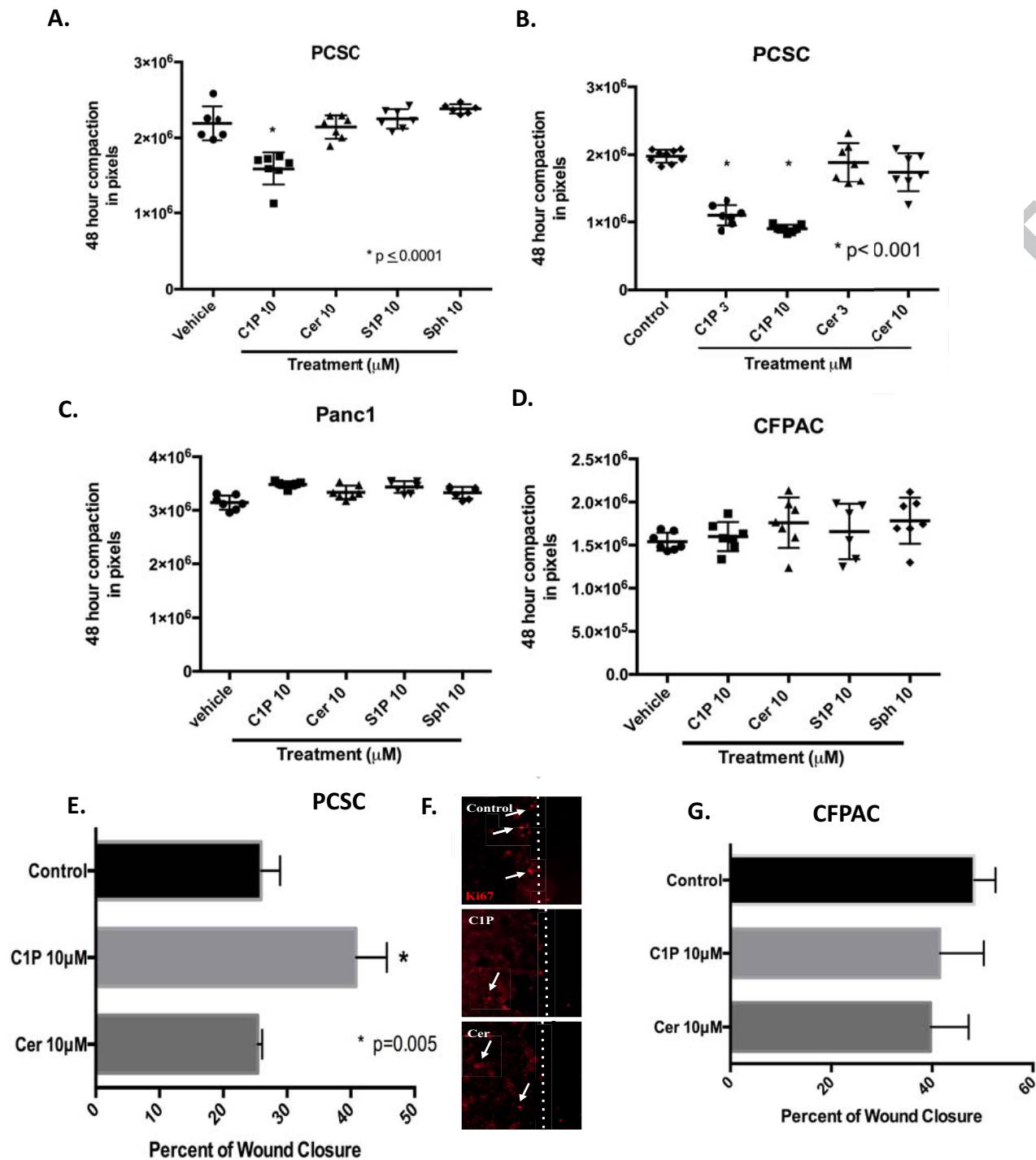


Figure 2: C1P mediated migration is selective to pancreatic cancer stem cells. Single cell suspensions of PCSC, CFPAC, and PANC1 in three-dimensional screening migration assay were assessed for aggregation at 48 hours with a decreased diameter reflecting a more compact spheroid and enhanced migration (measured as pixels). PCSC treated with C1P exhibited significant compaction (B, 3 μM : $1.09 \times 10^6 \pm 5.66 \times 10^4$ SEM pixels and 10 μM : $9.01 \times 10^5 \pm 2.1 \times 10^4$ SEM pixels) ($p \leq 0.0001$) (unpaired Student's t-test, $n=10$ /condition/experiment performed a minimum of 5 times) as compared to vehicle ($1.97 \times 10^6 \pm 3.17 \times 10^4$ SEM pixels). Compaction was specific to C1P as ceramide (cer) (A, 10 μM : $2.14 \times 10^6 \pm 5.79 \times 10^4$ SEM pixel, B, 3 μM : $1.88 \times 10^6 \pm 10.8 \times 10^4$ SEM pixels and 10 μM : $1.73 \times 10^6 \pm 10.6 \times 10^4$ SEM pixels), S1P (A, 10 μM : $2.25 \times 10^6 \pm 4.8 \times 10^4$ SEM pixels) or sphingosine (Sph) (A, 10 μM : $2.38 \times 10^6 \pm 2.5 \times 10^4$ SEM pixels) had no impact on PCSC aggregation. C1P had no impact on Panc1 or CFPAC cell aggregation (C, D respectively). Confluent monolayers subjected to in vitro scratch assay were assessed for wound closure at 24 hours. PCSC treated with C1P had a 41% (E, 10 μM : $41\% \pm 2.7$ SEM closure) ($p=0.005$) (ANOVA with post-hoc comparison, $n=3$ /condition/experiment performed a minimum of 5 occasions) as compared to vehicle (E, $26\% \pm 1.7$ SEM closure) and ceramide (10 μM : $25\% \pm 0.4$ SEM closure). Ki67 immunofluorescence staining (Cy3) at woundleading edge (white dotted line) supports wound closure in C1P treated cells is predominately due to migration (F). C1P and ceramide had no impact on CFPAC wound closure (G).

Figure 3

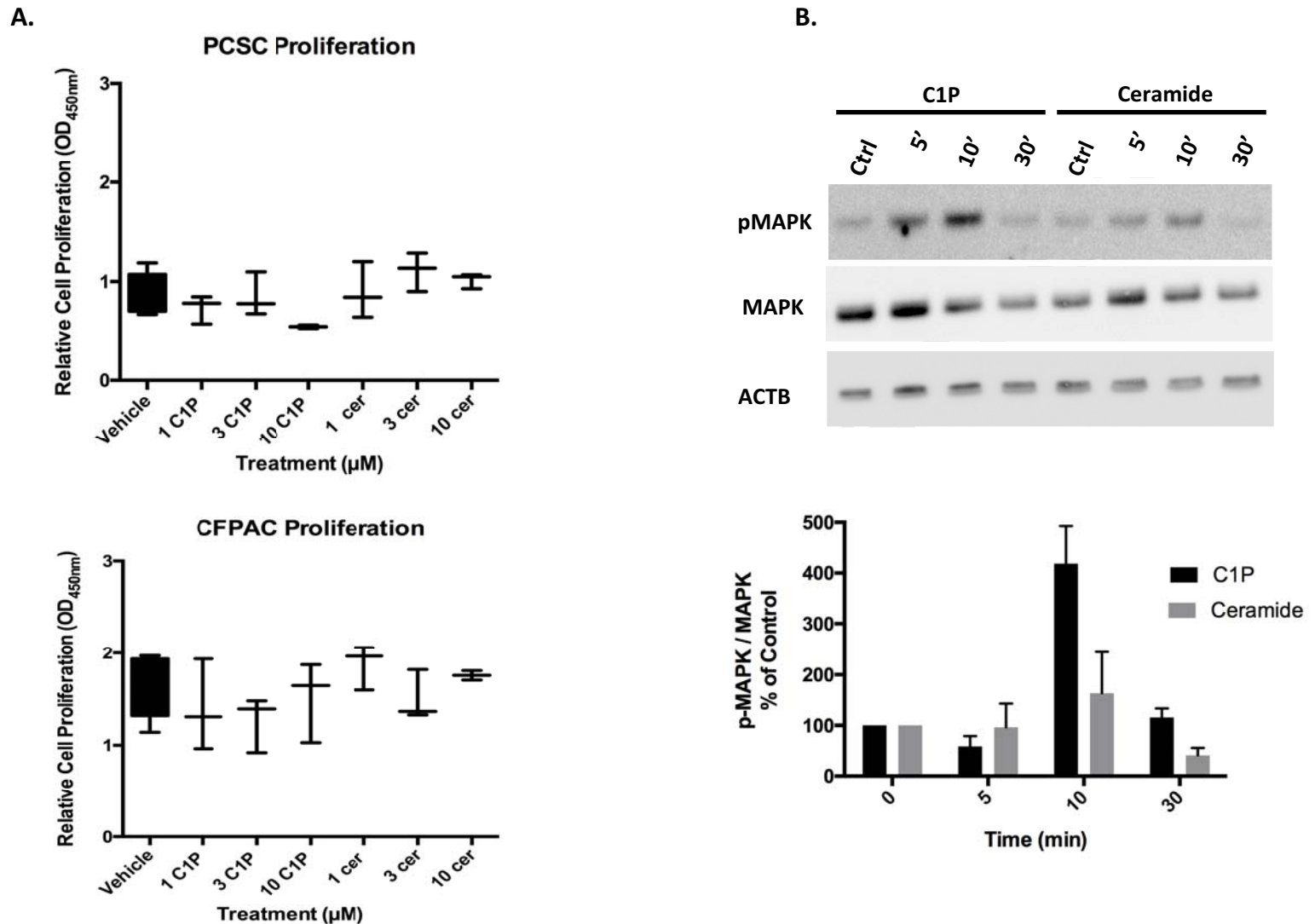


Figure 3: C1P had no impact on CSC or CFPAC proliferation, but does induce MAPK phosphorylation in CSC cells. Proliferation using WST in subconfluent CSC or CFPAC cells was not influenced by C1P (1-10 μM) or ceramide (1-10 μM) (A). Subconfluent PCSC cells were assessed for phosphorylation of MAPK overtime determined that C1P selectively induced significant phosphorylation as compared to ceramide (B, n=3, three different occasions, $p=0.0003$, Two-way ANOVA).

Figure 4:

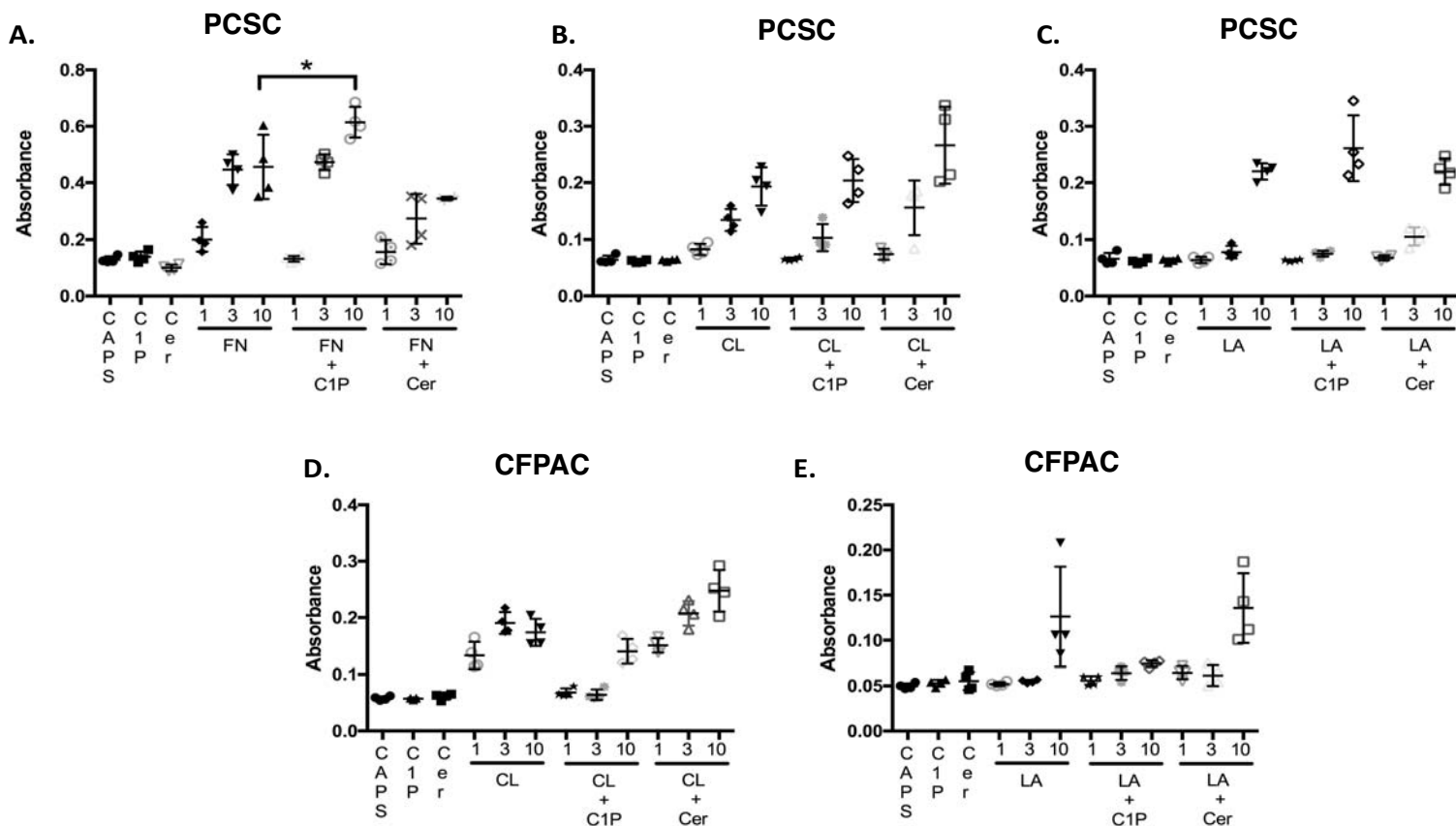


Figure 4: C1P increases FN-mediated PCSC adhesion. Wells coated with fibronectin (FN, 1-10 μ M), collagen (CL, 1-10 μ M), laminin (LA, 1-10 μ M), or vehicle (CAPS) as indicated while some wells were dual-coated with C1P (10 μ M) or ceramide (10 μ M). PCSC or CFPAC cells were seeded on pre-coated plates and adherent cells identified by crystal violet staining. PCSC cells demonstrated dose-dependent adhesion to FN (A), CL (B) and LA (C). CFPAC cells were non-adherent to FN (data not shown) but demonstrated a dose-dependent adhesion to CL (D). C1P significantly enhanced PCSC adhesion to 10 μ M FN (A, 0.6145 ± 0.0272 SEM) ($p=0.04$, $n=4$ /condition/experiment performed a minimum of 4 occasions) as compared to 10 μ M FN alone (0.4563 ± 0.0570 SEM) or ceramide \pm 10 μ M FN (0.3440 ± 0.0032 SEM).

Figure 5:

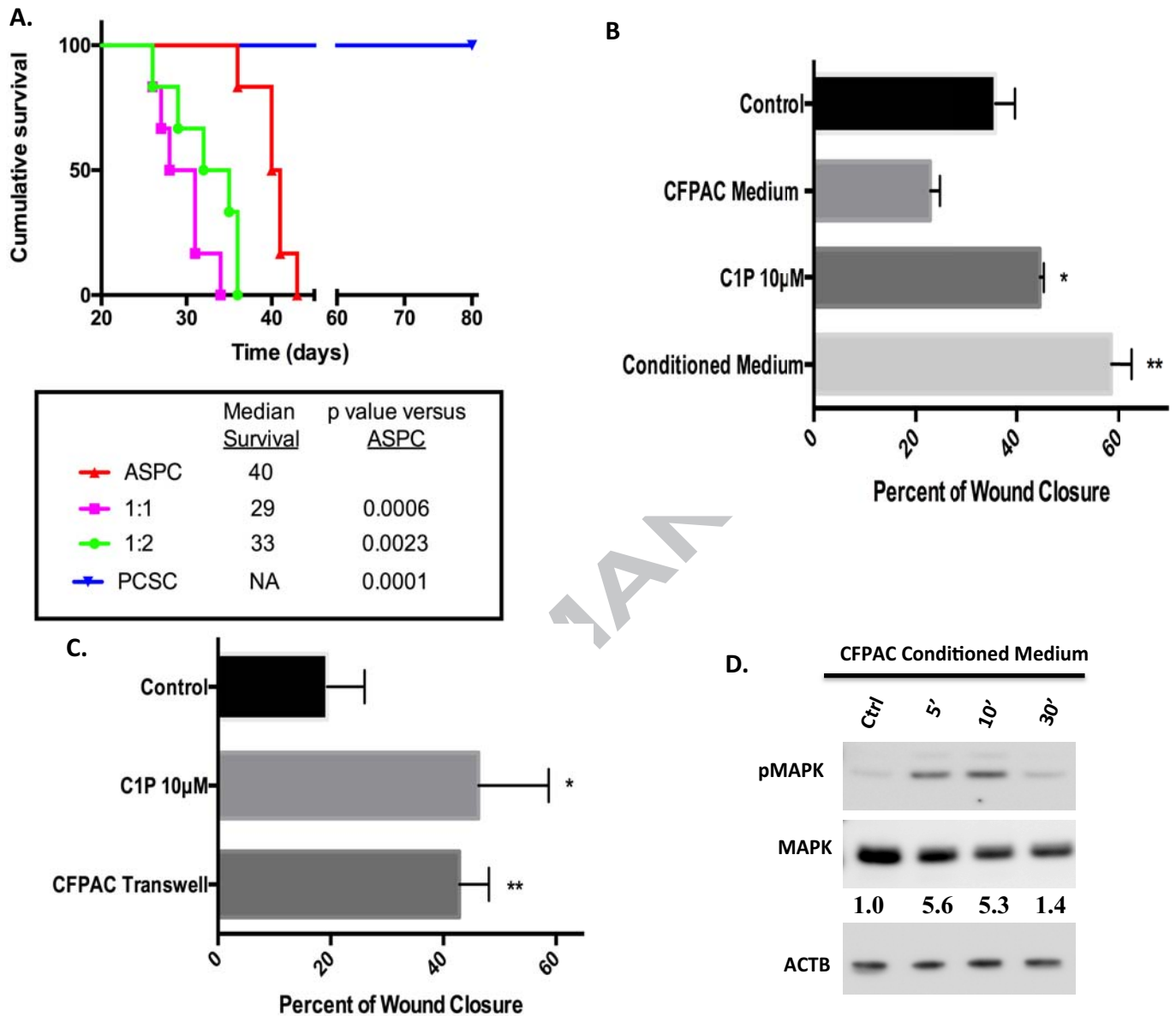


Figure 5: CSCs co-injected with AsPC-1 cells reduces animal survival while CFPAC conditioned medium and CFPAC in transwells increased CSC migration. Studies using AsPC-1 cells (0.75×10^6), AsPC-1 (0.75×10^6), + CSC cells (0.75×10^6), AsPC-1 (0.75×10^6), + CSCs (1.5×10^6), or CSCs alone (0.75×10^6) were injected intraperitoneally into NOD/SCID mice. Survival from was noted from time of tumor cell injection. Statistical group differences in survival time were calculated using log rank testing (Mantel-Cox) with reduction in survival noted in combined injected cell populations PCSC / AsPC-1 (1:1- $p=0.0006$ and 1:2- $p=0.0023$) as compared to AsPC-1 cells alone (A). Study was concluded on day 80 with no loss of CSC injected animals ($p=0.0001$, A) ($n=6$ /group). Consistent with C1P enhanced migration (A, $*p=0.0184$, $45\% \pm 0.43$ SEM), CSCs treated with CFPAC-conditioned medium (B, $**p=0.0025$, $59\% \pm 2.5$ SEM) significantly increased wound closure in CSC scratch assays as compared to unconditioned CFPAC medium ($23\% \pm 1.1$ SEM) or control medium ($36\% \pm 2.2$ SEM) (B, $n=3$ /condition/experiment performed a minimum of 4 occasions). Transwell co-culture of CFPAC cells with wounded CSCs significantly enhanced wound closure (B, $**p=0.471$, $43\% \pm 2.6$ SEM) consistent with that seen with C1P (B, $*p=0.0035$, $46\% \pm 6.2$ SEM) as compared to control (C, $19\% \pm 3.3$ SEM) ($n=4$ /condition/experiment performed a minimum of 3 occasions). CFPAC-conditioned medium induced a similar pattern of MAPK phosphorylation with densitometry analysis indicating a 5-fold increase in pMAPK (D, $n=2$, two different occasions, representative blot).

Figure 6

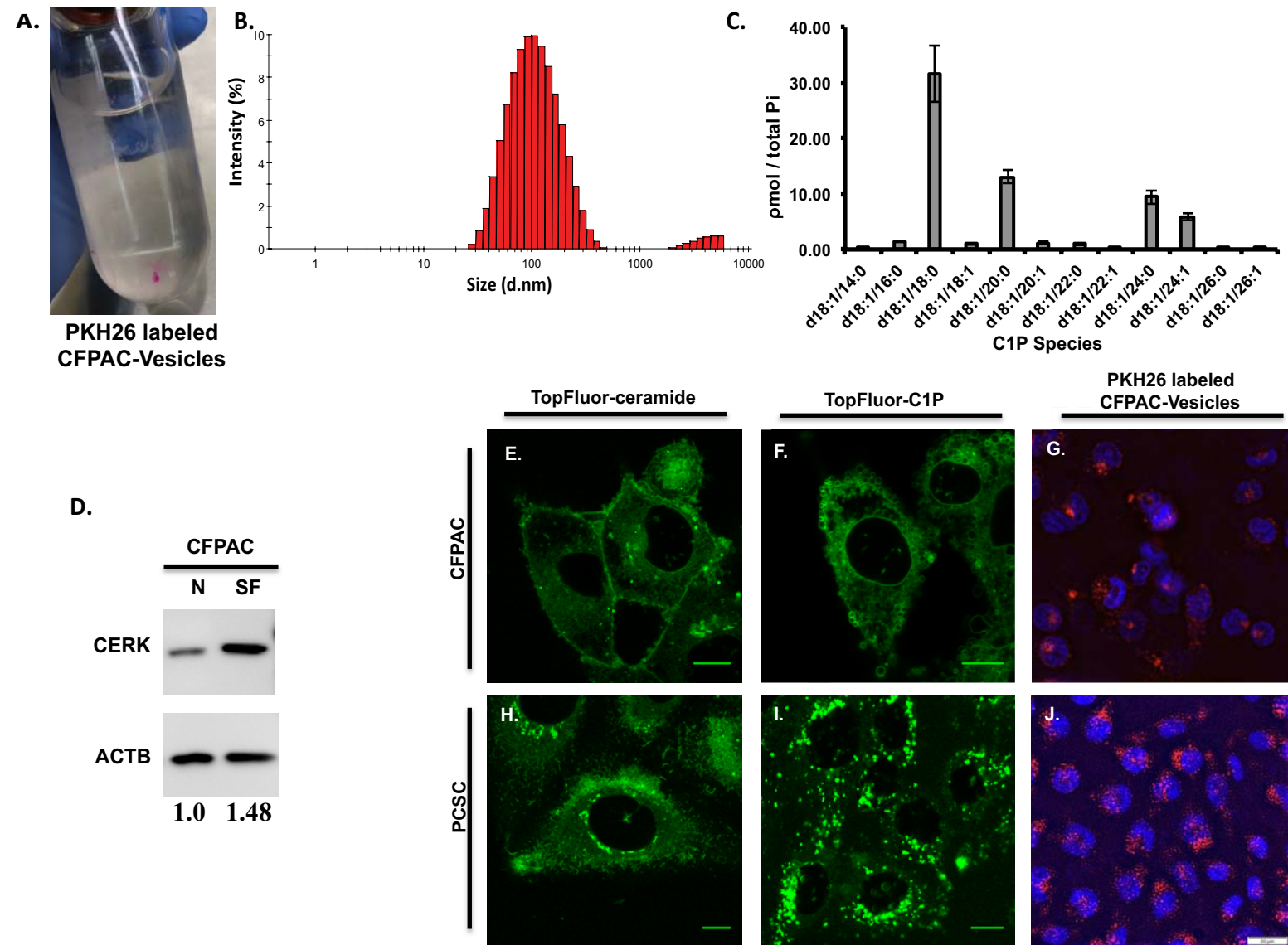
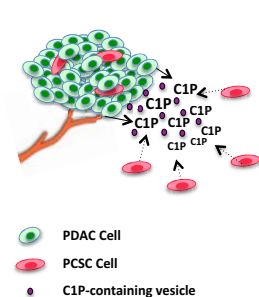


Figure 6: Extracellular vesicles secreted in CFPAC-conditioned medium are rich in C1P and C1P uptake is peri-nuclear in progenitor cells and is similar to uptake of CFPAC secreted C1P-containing extracellular vesicles.

The size of vesicles isolated using a sucrose gradient from CFPAC conditioned medium were assessed using Dynamic Light Scattering (DLS) where 95.88% were found to be $116\text{nm} \pm 3.5\text{ SEM}$ in size while the remaining 4.125% were $4219\text{nm} \pm 11.7\text{ SEM}$ (B) ($n=4$ unique preparations, 3 runs per preparation and a minimum of 12 measurements per run for a total of 144 measurements). Secreted vesicle isolates from serum-free (SF) CFPAC cells were noted to contain C1P species consistent with that seen in whole cell lysate (normalized to total phosphate: Pi, nmole/sample) (C). CFPAC cells in serum-free (SF) medium by densitometry analysis have a 1.48 fold increase in CERK compared to cells in normal medium (N) (D, $n=2$, representative blot). TopFluor labeled ceramide and C1P lipid uptake in sub-confluent PCSC and CFPAC cells. PCSCs exhibit a marked increase in C1P uptake in the perinuclear region (I) as compared to CFPAC (F) or TopFluor-ceramide (H,E). Conditioned medium from CFPAC cells was collected; extracellular vesicles isolated and surfaced labeled (A, PKH26 red fluorescent dye) and added to subconfluent cells ($n=3$ on different occasions). Perinuclear uptake of extracellular vesicles was significantly greater in PCSCs (J) as compared to CFPAC cells (G) (G,J: DAPI staining denotes nucleus) ($n=3$ on different occasions). Scale bar: $10\mu\text{m}$ (E,F,H,I), $20\mu\text{m}$ (G,J).

Pancreatic Adenocarcinoma



C1P rich PDAC cells release C1P-containing vesicles that impact migration and adhesion of PCSC cells.